Correction

NEUROSCIENCE

Correction for "A natural product inhibits the initiation of α-synuclein aggregation and suppresses its toxicity," by Michele Perni, Céline Galvagnion, Alexander Maltsev, Georg Meisl, Martin B. D. Müller, Pavan K. Challa, Julius B. Kirkegaard, Patrick Flagmeier, Samuel I. A. Cohen, Roberta Cascella, Serene W. Chen, Ryan Limboker, Pietro Sormanni, Gabriella T. Heller, Francesco A. Aprile, Nunilo Cremades, Cristina Cecchi, Fabrizio Chiti, Ellen A. A. Nollen, Tuomas P. J. Knowles, Michele Vendruscolo, Adriaan Bax, Michael Zasloff, and Christopher M. Dobson, which appeared in issue 6, February 7, 2017, of *Proc Natl Acad Sci USA* (114:E1009–E1017; first published January 17, 2017; 10.1073/pnas.1610586114).

The authors note that Ryan Limbocker's name incorrectly appeared as Ryan Limboker. The corrected author line appears below. The online version has been corrected.

Michele Perni, Céline Galvagnion, Alexander Maltsev, Georg Meisl, Martin B. D. Müller, Pavan K. Challa, Julius B. Kirkegaard, Patrick Flagmeier, Samuel I. A. Cohen, Roberta Cascella, Serene W. Chen, Ryan Limbocker, Pietro Sormanni, Gabriella T. Heller, Francesco A. Aprile, Nunilo Cremades, Cristina Cecchi, Fabrizio Chiti, Ellen A. A. Nollen, Tuomas P. J. Knowles, Michele Vendruscolo, Adriaan Bax, Michael Zasloff, and Christopher M. Dobson

www.pnas.org/cgi/doi/10.1073/pnas.1701964114

A natural product inhibits the initiation of α-synuclein aggregation and suppresses its toxicity

Michele Perni[a,b], Céline Galvagnion[a,1], Alexander Maltsev[c], Georg Meisl[a], Martin B. D. Müller[a,b], Pavan K. Challa[a], Julius B. Kirkegaard[d], Patrick Flagmeier[a], Samuel I. A. Cohen[a], Roberta Cascella[e], Serene W. Chen[a], Ryan Limbocker[a], Pietro Sormanni[a], Gabriella T. Heller[a], Francesco A. Aprile[a], Nunilo Cremades[f], Cristina Cecchi[e], Fabrizio Chiti[e], Ellen A. A. Nollen[b], Tuomas P. J. Knowles[a], Michele Vendruscolo[a,2], Adriaan Bax[c,2], Michael Zasloff[g,2], and Christopher M. Dobson[a,2]

[a]Department of Chemistry, University of Cambridge, Cambridge CB2 1EW, United Kingdom; [b]University Medical Centre Groningen, European Research Institute for the Biology of Aging, University of Groningen, Groningen 9713 AV, The Netherlands; [c]Laboratory of Chemical Physics, National Institute of Diabetes and Digestive and Kidney Diseases, National Institutes of Health, Bethesda, MD 20892; [d]Department of Applied Mathematics and Theoretical Physics, University of Cambridge, Cambridge CB3 0WA, United Kingdom; [e]Department of Experimental and Clinical Biomedical Sciences, University of Florence, Florence 50134, Italy; [f]Biocomputation and Complex Systems Physics Institute (BIFI)-Joint Unit BIFI-IQFR (CSIC), University of Zaragoza, 50018 Zaragoza, Spain; and [g]MedStar–Georgetown Transplant Institute, Georgetown University School of Medicine, Washington, DC 20010

Edited by Gregory A. Petsko, Weill Cornell Medical College, New York, NY, and approved December 5, 2016 (received for review June 29, 2016)

The self-assembly of α-synuclein is closely associated with Parkinson's disease and related syndromes. We show that squalamine, a natural product with known anticancer and antiviral activity, dramatically affects α-synuclein aggregation in vitro and in vivo. We elucidate the mechanism of action of squalamine by investigating its interaction with lipid vesicles, which are known to stimulate nucleation, and find that this compound displaces α-synuclein from the surfaces of such vesicles, thereby blocking the first steps in its aggregation process. We also show that squalamine almost completely suppresses the toxicity of α-synuclein oligomers in human neuroblastoma cells by inhibiting their interactions with lipid membranes. We further examine the effects of squalamine in a *Caenorhabditis elegans* strain overexpressing α-synuclein, observing a dramatic reduction of α-synuclein aggregation and an almost complete elimination of muscle paralysis. These findings suggest that squalamine could be a means of therapeutic intervention in Parkinson's disease and related conditions.

Parkinson's disease | protein aggregation | amyloid formation | toxic oligomers | drug development

The aggregation of α-synuclein (Fig. 1*A*), an intrinsically disordered protein expressed at high levels in the brain, is closely associated with the pathogenesis of a variety of neurodegenerative disorders, collectively known as α-synucleinopathies, including Parkinson's disease (PD), dementia with Lewy bodies (DLB), and multiple-system atrophy (MSA) (1–7). It has been exceptionally challenging, however, to develop effective strategies to suppress the formation of α-synuclein aggregates and their associated toxicity (8, 9), because the mechanism of aggregation of this protein is extremely complex and highly dependent on environmental factors, such as pH, temperature, and contact with surfaces (10). In particular, it is well established that phospholipid binding can accelerate fibril formation (11); moreover, it has recently been shown that such acceleration occurs through the enhancement of the initial primary nucleation step in the aggregation process (12). In the light of this information, we decided to investigate whether compounds capable of altering the binding of α-synuclein to lipid membranes could be effective in inhibiting its aggregation. This study was stimulated by our recent finding that a small molecule, bexarotene, can suppress significantly the primary nucleation reaction that initiates the production of the $A\beta_{42}$ aggregates linked with Alzheimer's disease (AD) and reduces the associated toxicity in a *Caenorhabditis elegans* model of this disease (13).

In the present work, we have focused on one particular compound, squalamine (Fig. 1*B*), an antimicrobial aminosterol originally discovered in 1993 in the dogfish shark, *Squalus acanthias* (14). This small molecule, now prepared synthetically (see *SI Materials and Methods* for details), has been found to have pharmacological activity in endothelial cells by inhibiting growth factor-dependent pathways and thus has emerged as a drug candidate for the treatment of cancer and macular degeneration (15, 16). In the present context, our choice of studying squalamine was prompted by the observation that this molecule is able to enter eukaryotic cells and displace proteins that are bound to the cytoplasmic face of plasma membranes (17–19), suggesting that it may influence the initiation of the aggregation of α-synuclein (12). Indeed squalamine has been referred to as a "cationic lipid" (18) as it carries a net positive charge and shows a high affinity for anionic phospholipids (20) of the type that nucleates the aggregation of α-synuclein, thereby reducing the negative charge of the membrane surface to which it is bound (18, 21) without significantly disrupting the integrity of lipid surfaces (18). In analogy, it has recently been shown that a homologous protein, β-synuclein, can inhibit α-synuclein lipid-induced aggregation via a competitive binding at the surface of lipid vesicles (22).

Significance

Parkinson's disease is characterized by the presence in brain tissues of aberrant aggregates primarily formed by the protein α-synuclein. It has been difficult, however, to identify compounds capable of preventing the formation of such deposits because of the complexity of the aggregation process of α-synuclein. By exploiting recently developed highly quantitative in vitro assays, we identify a compound, squalamine, that blocks α-synuclein aggregation, and characterize its mode of action. Our results show that squalamine, by competing with α-synuclein for binding lipid membranes, specifically inhibits the initiation of the aggregation process of α-synuclein and abolishes the toxicity of α-synuclein oligomers in neuronal cells and in an animal model of Parkinson's disease.

Author contributions: M.P., E.A.A.N., T.P.J.K., M.V., A.B., M.Z., and C.M.D. designed research; M.P., C.G., A.M., G.M., M.B.D.M., P.K.C., J.B.K., P.F., R.C., R.L., P.S., G.T.H., F.A.A., C.C., F.C., T.P.J.K., A.B., and M.Z. performed research; P.K.C., S.W.C., N.C., and E.A.A.N. contributed new reagents/analytic tools; M.P., C.G., A.M., G.M., P.K.C., J.B.K., P.F., S.I.A.C., R.C., R.L., P.S., C.C., F.C., E.A.A.N., T.P.J.K., A.B., M.Z., and C.M.D. analyzed data; and M.P., T.P.J.K., M.V., A.B., M.Z., and C.M.D. wrote the paper.

Conflict of interest statement: M.Z. is the inventor on a patent application that has been filed related to the compound described in this paper. The other authors declare no conflict of interest.

This article is a PNAS Direct Submission.

Freely available online through the PNAS open access option.

See Commentary on page 1223.

[1]Present address: German Center for Neurodegenerative Diseases (DZNE), 53127 Bonn, Germany, and Institute of Physical Biology, Heinrich Heine Universität, Universitätsstr. 1, 40225 Duesseldorf, Germany.

[2]To whom correspondence may be addressed. Email: mv245@cam.ac.uk, bax@nih.gov, maz5@georgetown.edu, or cmd44@cam.ac.uk.

This article contains supporting information online at www.pnas.org/lookup/suppl/doi:10.1073/pnas.1610586114/-/DCSupplemental.

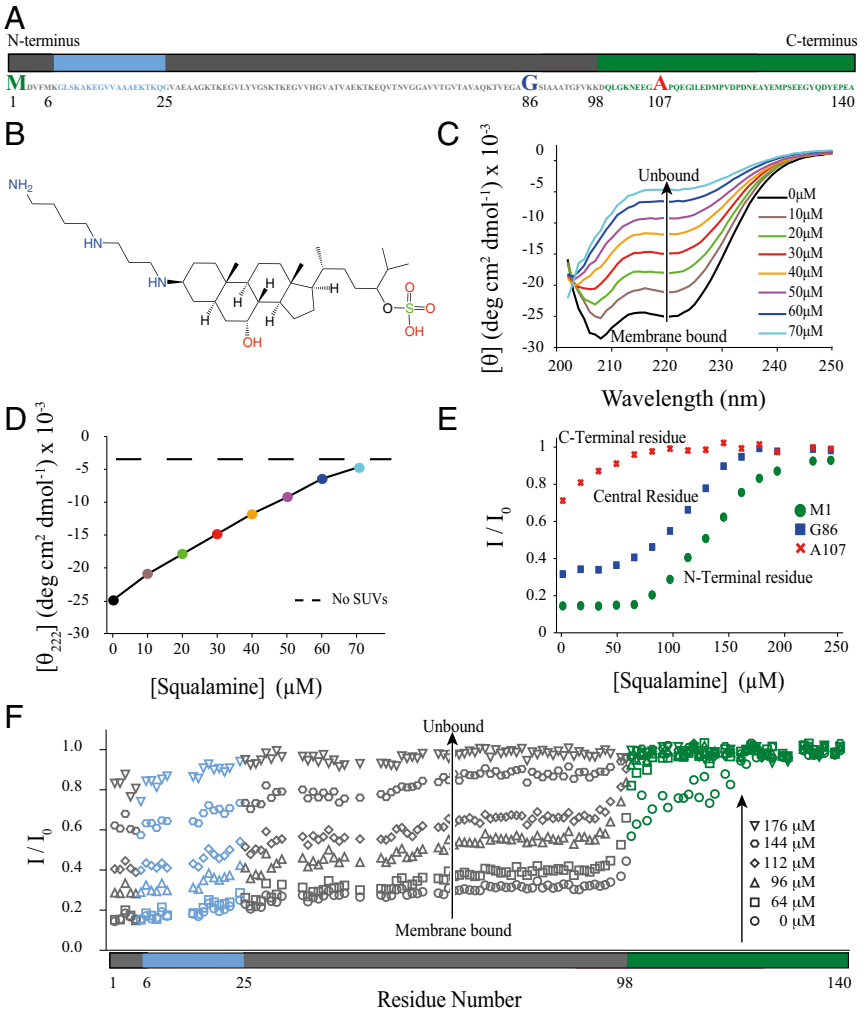

Fig. 1. Squalamine displaces α-synuclein from DOPS:DOPE:DOPC (30:50:20) vesicles. (*A*) Amino acid sequence of α-synuclein and its three distinct regions (44), the N-terminal region (blue), the central region (gray), and the C-terminal fragment (green). (*B*) Structure of squalamine (21). (*C* and *D*) Changes in the CD spectrum (*C*) and the mean residue ellipticity (MRE) (*D*) at 222 nm of 5 μM α-synuclein in the presence of 1.25 mM DOPS:DOPE:DOPC (30:50:20) vesicles in the absence (black) and presence (colors) of increasing concentrations of squalamine: 10 μM (brown), 20 μM (green), 30 μM (red), 40 μM (orange), 50 μM (violet), 60 μM (blue), and 70 μM (light blue) in 20 mM Tris (pH 7.4) and 100 mM NaCl. The dashed horizontal line in *D* indicates the MRE at 222 nm of monomeric α-synuclein in the absence of lipids. Nearly complete displacement of α-synuclein is achieved for a lipid:squalamine ratio of about 18:1. (*E*) Ratios of the α-synuclein NMR peak heights as a function of added squalamine for three residues representative of the three regions of α-synuclein with distinct forms of behavior (11), the N-terminal residue M1 (circles), the central non-Aβ component (NAC) residue G86 (squares), and the C-terminal residue A107 (crosses). (*F*) Ratios of the NMR peak heights of 100 μM of α-synuclein observed in ^{1}H-^{15}N NMR HSQC spectra in the presence of DOPE:DOPS:DOPC (30:50:20) vesicles (1.25 mM) and different concentrations of squalamine (0 μM, circles; 64 μM, squares; 96 μM, triangles; 112 μM, rhomboids; 144 μM, hexagons; and 176 μM, inverted triangles) relative to peak heights in a spectrum of α-synuclein in the absence of lipids and squalamine. Essentially complete displacement of α-synuclein from lipid membranes is observed at a concentration of squalamine of ca. 200 μM, corresponding to a lipid:squalamine ratio of about 6:1. For all the experiments shown in this figure N-terminally acetylated α-synuclein was used (45).

Because of these properties, we investigated the possibility that squalamine could be effective in interfering with the membrane-induced aggregation of α-synuclein. We first investigated the possible mechanism of action of squalamine in this regard by detailed biophysical studies in vitro and extended those results by testing the effects of squalamine on the toxicity of α-synuclein oligomers, using human neuroblastoma cells in culture (23, 24), and then carried out experiments in vivo, using a well-established *C. elegans* animal model of PD (25).

Results

Squalamine Displaces α-Synuclein from Lipid Membranes. To study whether or not squalamine can affect the binding of α-synuclein to lipid bilayers, we first used small unilamellar vesicles (SUVs) with diameters of about 30 nm composed of 30% 1,2-dioleoyl-*sn*-glycero-3-phospho-L-serine (DOPS), 50% 1,2-dioleoyl-*sn*-glycero-3-phosphoethanolamine (DOPE), and 20% 1,2-dioleoyl-*sn*-glycero-3-phosphocholine (DOPC), which represent the most abundant lipids found in the membranes of synaptic vesicles (26). Titrating squalamine into a solution of α-synuclein bound to DOPS:DOPE:DOPC (30:50:20) vesicles was observed to reduce the α-helical content of α-synuclein in an approximately linear manner with squalamine concentration, as measured by circular dichroism (CD) (Fig. 1 *C* and *D*). This observation suggests that squalamine is able to displace α-synuclein from the surface of lipid bilayers.

The physiological concentration of α-synuclein in neuronal synapses is estimated to be about 50 μM (27, 28), a concentration of protein that can be studied by NMR spectroscopy (27, 29–32). We therefore used this technique to probe potential interactions between α-synuclein and squalamine in the absence of lipids and to

characterize the displacement of the protein from lipid membranes by squalamine, as suggested by the CD experiments. This approach is based on the fact that even very weak interactions typically generate measurable shifts in the NMR signals of interacting molecules and often broaden the resonances to an extent that is determined by the rates involved in the binding process.

We first incubated free monomeric α-synuclein in the absence of lipids and in the presence of increasing concentrations of

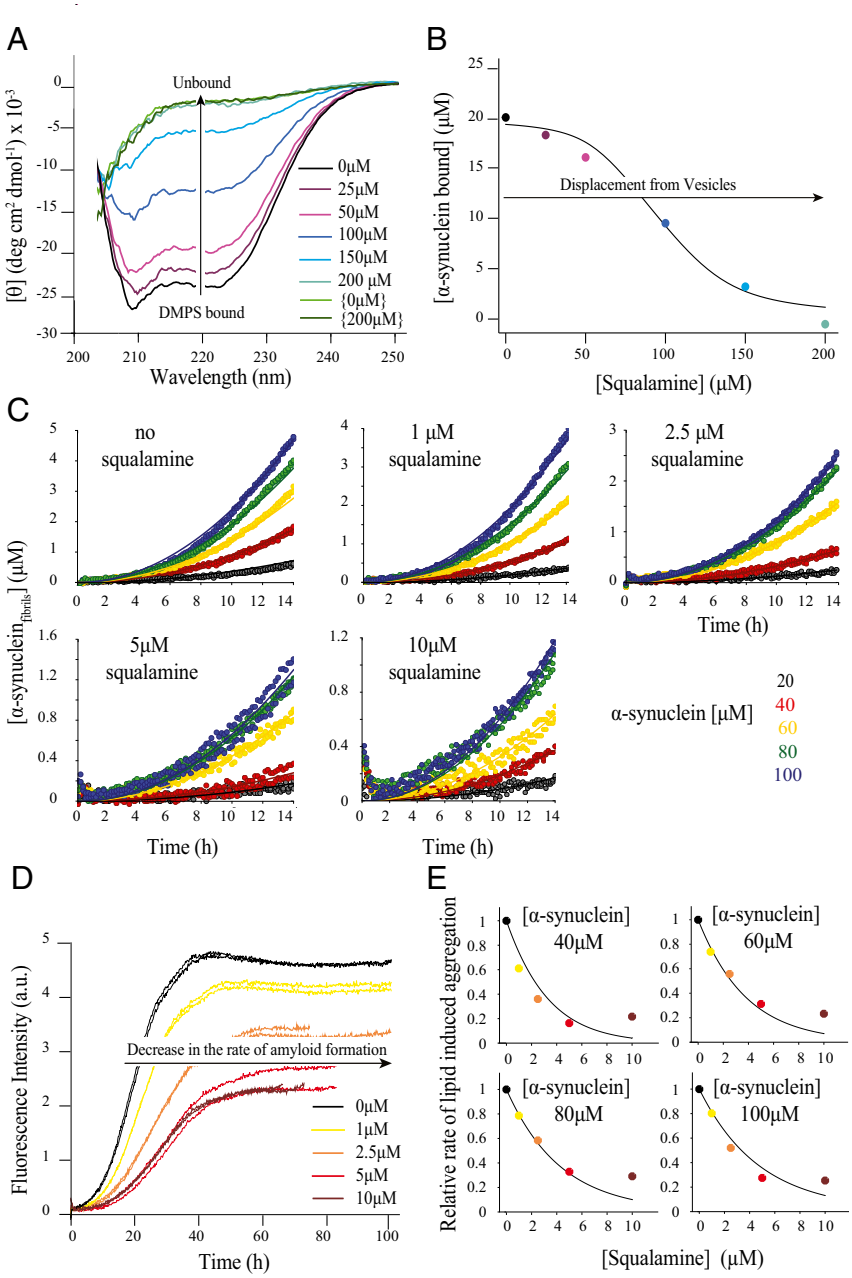

Fig. 2. Squalamine inhibits α-synuclein aggregation via competitive binding with lipid membranes. (*A*) Changes in the CD spectrum of 20 μM α-synuclein in the presence of 1 mM DMPS and in the absence (black) or presence (colors) of increasing concentrations of squalamine: 25 μM (violet), 50 μM (pink), 100 μM (blue), 150 μM (light blue), and 200 μM (aqua). The spectrum of α-synuclein in the absence of both DMPS and squalamine is shown in light green and the CD spectrum of α-synuclein in the absence of DMPS and the presence of 200 μM squalamine is shown in dark green. Essentially complete displacement of the protein from the membrane was observed for a squalamine:lipid ratio of about 1:5. (*B*) Changes in the concentration of α-synuclein bound to DMPS vesicles with increasing concentrations of squalamine. The data are well described by a competitive binding model with $K_{D,\alpha}$ and L_α [0.5 μM and 30 μM, respectively (12)], and the fit yields $K_{D,S}$ = 67 nM and L_S = 7.3, respectively (see *SI Materials and Methods* for details). (*C*) Global fits of the early time points in the kinetic traces of α-synuclein aggregation at increasing concentrations of squalamine. For each dataset, the concentration of DMPS is 100 μM and that of α-synuclein is 20 μM (black), 40 μM (red), 60 μM (yellow), 80 μM (green), and 100 μM (blue). The squalamine concentration used was 0 μM, 1 μM, 2.5 μM, 5 μM, and 10 μM. (*D*) Changes in thioflavin-T (ThT) fluorescence when 100 μM α-synuclein was incubated with 100 μM DMPS vesicles in the presence of increasing concentrations of squalamine: 0 μM (black), 1 μM (yellow), 2.5 μM (orange), 5 μM (red), and 10 μM (brown). All data were acquired under quiescent conditions at 30 °C and duplicate runs are shown. (*E*) Variation in the relative rate of lipid-induced aggregation of α-synuclein with increasing concentrations of squalamine (0 μM, black; 1 μM, yellow; 2.5 μM, orange; 5 μM, red; and 10 μM, brown). The solid line is the corresponding global fit using a competitive binding model (See *SI Materials and Methods* for details) with only one free parameter, n_b (the reaction order of the lipid-induced aggregation with respect to the fraction of the protein bound), which was found to be 5.5.

squalamine and observed small chemical shift changes in the resonances of residues in the C-terminal region of the protein (Fig. S1), consistent with those associated with the weak binding of α-synuclein to other polyamine compounds (33). The interaction involves two regions between residues 85 and 140, where the NMR spectra reveal two distinct types of behavior; the resonances of residues 88–106 show only very small effects, but those of residues 113–139 are affected in a much more pronounced manner. To probe the stoichiometry of the interaction of α-synuclein and squalamine and to estimate the binding constant, we performed a series of dilutions on a sample containing 80 μM α-synuclein and 240 μM squalamine, monitoring the intensities of the α-synuclein resonances (Fig. S1). This experiment shows that when the squalamine concentration becomes lower than about 100 μM, the spectral changes characteristic of the interaction are no longer visible.

Then, we investigated further the displacement of α-synuclein from the membrane by squalamine. It has been previously demonstrated that addition of DOPE:DOPS:DOPC (50:30:20) vesicles to a sample of α-synuclein results in attenuation of the main-chain amide signals of its about 100 N-terminal residues in the ^{1}H-^{15}N heteronuclear single quantum correlation (HSQC) NMR spectrum (27). This attenuation is attributable to the binding of these residues to the large, slowly tumbling vesicles, whereas the secondary structure becomes α-helical, as indicated by CD measurements and by indirect transferred nuclear Overhauser effects (NOEs) in the spectra (27). By contrast, the resonances of the 40 C-terminal residues retain almost their full intensity and experience only very minor changes in chemical shifts (Fig. 1*F*). In the present work we prepared an NMR sample containing a sufficient quantity of lipid vesicles to cause a large attenuation of the signals of α-synuclein and then titrated increasing amounts of squalamine into the sample (Fig. 1 *E* and *F*). We observed that the addition of about 200 μM of squalamine resulted in an almost complete recovery of the intensity of the α-synuclein signals (Fig. 1*F*) and found that signals from residues 101–120, which are affected to a much smaller extent than residues 1–100 by the presence of lipids, were restored to their free intensities at a much lower concentration of squalamine.

Interestingly, even though the squalamine:α-synuclein ratios and the absolute squalamine concentrations in the presence of DOPE:DOPS:DOPC vesicles (Fig. 1 *C* and *D*) were comparable to those in the lipid-free experiments (Fig. S1), there was no evidence in the former experiments for the interaction of squalamine with the C-terminal residues. In addition, when the squalamine concentration was increased to 80 μM in the absence

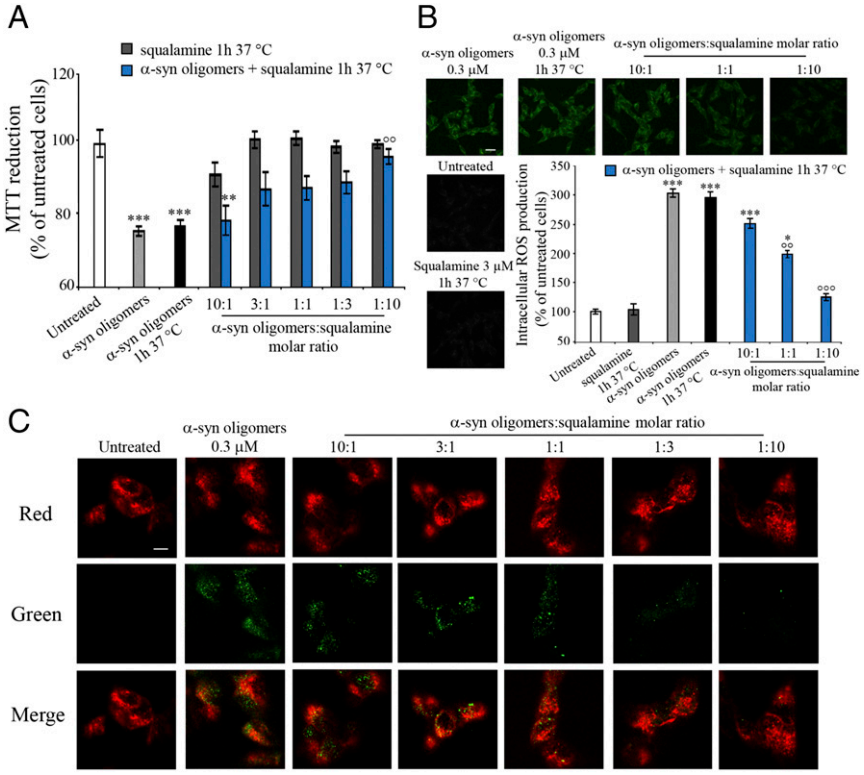

Fig. 3. Squalamine suppresses the toxicity of α-synuclein oligomers in human neuroblastoma cells by inhibiting their binding to the cell membranes. (*A*) Effects of squalamine on α-synuclein oligomer-induced MTT reduction in SH-SY5Y cells. α-Synuclein oligomers (23, 24) were resuspended in the cell culture medium at a concentration of 0.3 μM, incubated with or without increasing concentrations (0.03 μM, 0.1 μM, 0.3 μM, 1.0 μM, and 3.0 μM) of squalamine for 1 h at 37 °C under shaking conditions, and then added to the cell culture medium of SH-SY5Y cells for 24 h. The cells were also treated with squalamine preincubated in the absence of oligomers for 1 h at 37 °C under shaking conditions. $^{**}P \leq 0.01$ and $^{***}P \leq 0.001$, respectively, relative to untreated cells and $^{\circ\circ}P \leq 0.01$ relative to cells treated with α-synuclein oligomers. (*B*) Representative confocal scanning microscope images of SH-SY5Y cells showing the effect of squalamine on α-synuclein oligomer-induced ROS production. α-Synuclein oligomers were resuspended in the cell culture medium at a concentration of 0.3 μM, incubated with or without increasing concentrations (0.03 μM, 0.3 μM, and 3.0 μM) of squalamine for 1 h at 37 °C under shaking conditions, and then added to the cell culture medium of SH-SY5Y cells for 15 min. The cells were also treated with 3 μM squalamine preincubated without oligomers for 1 h at 37 °C while shaking. The green fluorescence arises from the 2′,7′-dichlorodihydrofluorescein diacetate (CM-H_2DCFDA) probe that has reacted with ROS. (Scale bar, 30 μm.) $^{*}P \leq 0.05$, $^{**}P \leq 0.01$, and $^{***}P \leq 0.001$, respectively, relative to untreated cells. $^{\circ\circ}P \leq 0.01$ and $^{\circ\circ\circ}P \leq 0.001$, respectively, relative to untreated cells and the symbol °° indicates $P \leq 0.01$ relative to cells treated with α-synuclein oligomers. (*C*) Representative confocal scanning microscopy images of the apical sections of SH-SY5Y cells treated for 15 min with α-synuclein oligomers (0.3 μM) and increasing concentrations (0.03 μM, 0.1 μM, 0.3 μM, 1.0 μM, and 3.0 μM) of squalamine. Red and green fluorescence indicates the cell membranes and the α-synuclein oligomers, respectively. (Scale bar, 10 μm.)

of α-synuclein, the sample became highly opaque, suggesting that the lipid vesicles in the sample undergo fusion within seconds, an effect likely to be due to the change in the electrostatic properties of the lipid vesicles upon squalamine binding. However, in the presence of α-synuclein the samples were stable and no precipitation occurred within the time scales of either the CD or the NMR experiments.

Taken together, these observations demonstrate that, in a system containing α-synuclein and negatively charged lipid membranes, squalamine partitions to the membrane surface, thereby inducing the displacement of the protein from the membrane rather than remaining free in solution and interacting directly with α-synuclein.

Squalamine Inhibits Lipid-Induced Aggregation of α-Synuclein by Competing for Binding Sites at the Surface of the DMPS Vesicles. In the light of these results, we explored the effects of squalamine on the binding and aggregation of α-synuclein in the presence of 1,2-dimyristoyl-sn-glycero-3-phospho-L-serine (DMPS)-containing vesicles, which have been shown to be particularly effective in enhancing the rate of aggregation and amyloid formation by α-synuclein (12). We first incubated the protein under conditions where effectively all of the α-synuclein molecules present in the sample were bound to the vesicles and in the presence of increasing concentrations of squalamine. As observed in the experiments with the DOPS:DOPE:DOPC (30:50:20) vesicles (Fig. 1 *C*–*F*), the presence of squalamine progressively decreased the α-helical content of α-synuclein (Fig. 2*A*), again indicating that squalamine displaces the protein from the vesicles. We thus used the same competitive binding model (Fig. 2*B*) as the one describing the displacement of α-synuclein from the vesicle by β-synuclein (22), where both α-synuclein and squalamine compete for binding sites at the surface of the DMPS vesicles, in order to analyze the CD data. This model, together with previously determined binding constants for the α-synuclein/DMPS system (12), described the data very closely and yielded values for both the binding constant and the stoichiometry of the binding of squalamine to DMPS vesicles, $K_{D,S} = 67$ nM and $L_S = 7.3$, respectively. These results suggest that the positively charged squalamine binds strongly to the anionic head groups of the lipid bilayers, progressively coating the surfaces of the lipid membrane, thereby decreasing the electrostatic forces and competing for the sites on the lipid vesicles that are required for the binding of α-synuclein.

We further monitored the effects of increasing concentrations of squalamine on the size and the fluidity of the DMPS vesicles, using dynamic light scattering and differential scanning calorimetry (Fig. S2), respectively. The presence of squalamine caused an increase in the diameter of the DMPS vesicles from about 20 nm to values in excess of 100 nm at squalamine:lipid ratios greater than 0.1 (Fig. S2). In addition, differential scanning calorimetry

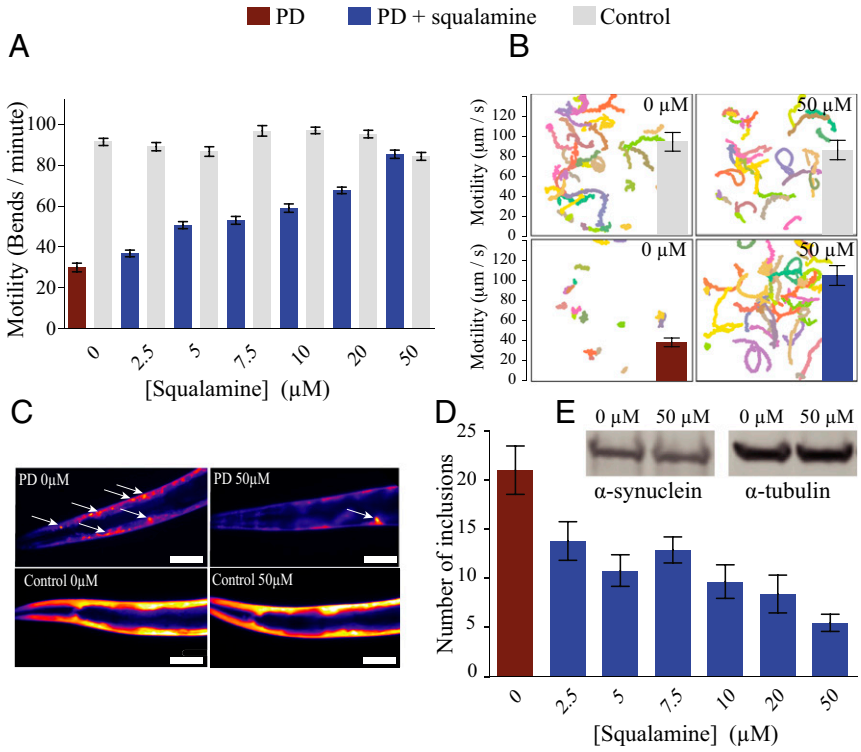

Fig. 4. Squalamine inhibits the formation of α-synuclein inclusions and the consequent muscle paralysis associated with the overexpression of this protein in a *C. elegans* model of PD. (*A*) Recovery of the normal phenotype at day 4 of adulthood for PD worms (red bars) and for worms expressing α-synuclein (blue bars) compared with control worms (gray bars) as the concentration of squalamine was raised to 50 μM. The data were obtained using an automated body bend assay; the plot shows one representative dataset of three independent experiments that gave very similar results. (*B*) Swimming tracks representative of the movement of PD and control worms over a time period of 1 min, without and with squalamine. Tracks corresponding to the movement of different animals are represented in different colors. The motility (speed of movement and body bends) of the PD worms can be seen to be greatly enhanced after exposure to 50 μM squalamine. Red bars, PD worms; blue bars, treated PD worms; gray bars, control worms. The error bars represent the SEM. (*C*) Representative images, showing a substantial decrease in the number of inclusions in PD worms in the presence of 50 μM squalamine, whereas the YFP expression pattern in control worms is not affected. All measurements were carried out at day 12 of adulthood. (Scale bars, 70 μm.) Inclusions are indicated with white arrows. (*D*) Reduction in the number of α-synuclein inclusions in PD worms, in the presence of squalamine. Fifty animals were analyzed in total. Red bar, PD worms; blue bars, treated PD worms. (*E*) Western blot analysis of protein extracts from day 12 PD worms showing similar expression levels of α-synuclein and α-tubulin (loading control) in the absence and presence of 50 μM squalamine.

(DSC) traces of the DMPS vesicles in the absence and presence of 50 μM squalamine show that the molecule induced a decrease in the melting temperature by 10 °C (Fig. S2), an effect similar to that observed upon binding of α-synuclein to DMPS vesicles (12), suggesting that squalamine interacts with the membrane surface. Overall, however, these results indicate that at squalamine:DMPS ratios below 1:10 the integrity of the vesicles is not compromised.

We then studied the aggregation of α-synuclein in the presence of DMPS vesicles and increasing concentrations of squalamine and observed that the overall rate of amyloid formation under such conditions decreases dramatically in a dose-dependent manner (Fig. 2 *C–E*). It is interesting to note that the observed change in the rate of lipid-induced aggregation of α-synuclein is not likely to be due to a change in the vesicle morphology; as discussed above, at the squalamine:lipid ratios used here the diameter of the vesicles ranges from 20 nm to 100 nm (Fig. S2), and this size variation has been shown not to affect significantly the kinetics of amyloid formation by α-synuclein in the presence of DMPS vesicles (12).

To quantify further the effects of squalamine on α-synuclein aggregation, we analyzed the early stages of the kinetic traces (Fig. 2*C*) (12) (see *SI Materials and Methods* for details) and determined the rate of α-synuclein aggregation at each concentration of squalamine (Fig. 2*E*). The change in the relative rate of lipid-induced aggregation of α-synuclein with increasing concentration of squalamine is well described by a competitive binding model, with the binding constants determined here for squalamine ($K_{D,S}$ and L_S) and previously for α-synuclein ($K_{D,\alpha}$ and L_α) (12). Taken together, these results are consistent with the conclusion that squalamine inhibits the lipid-induced aggregation of α-synuclein via competitive binding at the surfaces of the vesicles, as observed for β-synuclein (22). In addition, we probed the interaction of squalamine with α-synuclein fibrils by incubating squalamine in the presence of the fibrils. We then centrifuged the sample and separated the supernatant from the pellet. Then we assessed the quantity of squalamine in the supernatant before and after incubation with fibrils using, mass spectrometry (Fig. S3). We found that, after incubation, the signal corresponding to squalamine in the supernatant was reduced (−85%), suggesting a degree of binding to α-synuclein fibrils. This interaction may also play a role in the observed inhibition of squalamine on the lipid-induced aggregation of α-synuclein. As a control we performed the same experiment, using $A\beta_{42}$ fibrils (Fig. S3). In this case, we observed a lower binding signal (−66%), indicating stronger binding to α-synuclein fibrils.

Squalamine Suppresses the Toxicity of α-Synuclein Oligomers in Human Neuroblastoma Cell Lines by Inhibiting Their Binding to Cellular Membranes. We have recently developed a protocol to isolate oligomers of α-synuclein shown to be toxic to human cells (23, 24). We exposed cultured human SH-SY5Y neuroblastoma culture cells to such oligomers at a concentration of 0.3 μM (monomer equivalent of α-synuclein). Under these conditions, the oligomers were indeed toxic to the cells, as demonstrated by the decreased ability of the cells to chemically reduce 3-(4,5-dimethylthiazol-2-yl)-2,5-diphenyltetrazolium bromide (MTT) (Fig. 3*A*). The cells were also treated with α-synuclein oligomers (0.3 μM) in the presence of increasing concentrations of squalamine (up to 3.0 μM) (Fig. 3*A*). The results show that squalamine decreases markedly the mitochondrial damage induced by the α-synuclein

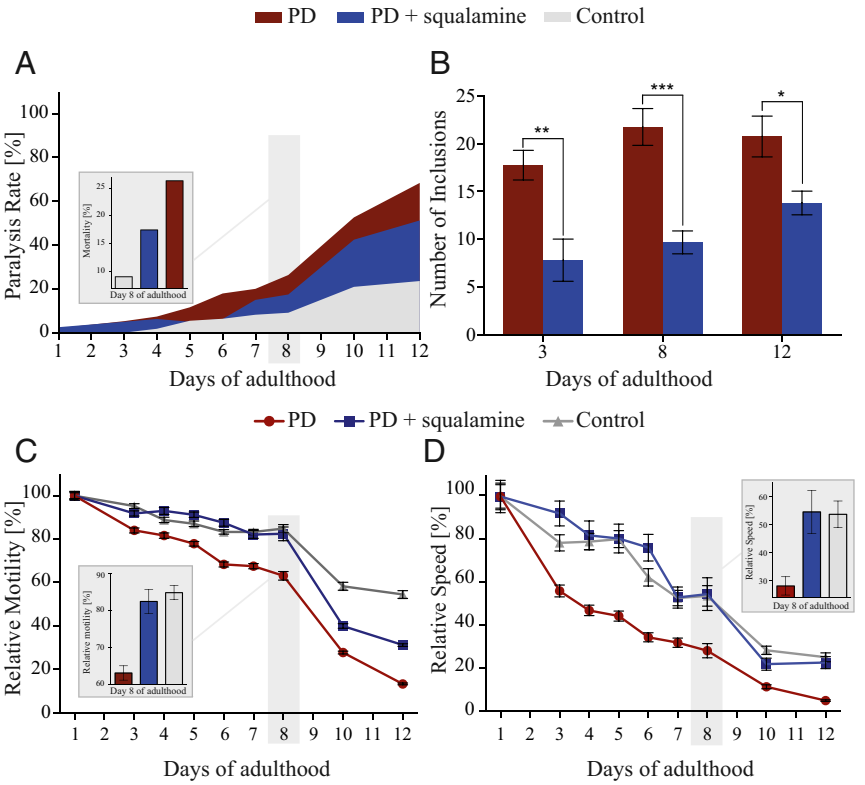

Fig. 5. Squalamine greatly improves the fitness of PD worms (25) and reduces α-synuclein aggregation over time. (*A*) The administration of 10 μM squalamine decreased substantially the paralysis rate of PD worms. Red, PD worms; blue, treated PD worms; gray, control worms. (*B*) The aggregation of α-synuclein in PD animals treated with 10 μM squalamine is greatly decreased compared with that in untreated worms; the plots show one representative of three experiments. Error bars represent the SEM. Red bars, PD worms; blue bars, treated PD worms. (*C* and *D*) Exposure to 10 μM squalamine greatly improves the thrashing (*C*) and speed (*D*) of the PD worms over 12 d. *Insets* show details of relative motility, thrashing, and speed, respectively, for day 8. Red lines, PD worms; blue lines, treated PD worms; gray lines, control worms.

oligomers, as indicated by MTT reduction data, with the protective effect increasing with squalamine concentration (Fig. 3*A*). Similar results were obtained from analyzing intracellular reactive oxygen species (ROS) production within SH-SY5Y cells; the α-synuclein oligomers (0.3 μM) induced a sharp increase in ROS levels in this cell model, indicating increased ROS-induced cellular damage (Fig. 3*B*). Upon treatment of the cells with α-synuclein oligomers (0.3 μM monomer equivalent) and increasing concentrations (0.03 μM, 0.3 μM, and 3 μM) of squalamine, the degree of ROS-derived fluorescence was observed to decrease steadily with increasing squalamine concentration (Fig. 3*B*), and at the highest ratio of squalamine:α-synuclein concentrations it was found to suppress almost completely the increase of intracellular ROS levels caused by the oligomers.

We then investigated the mechanism by which squalamine inhibits α-synuclein oligomer toxicity by analyzing the interactions between the oligomers (0.3 μM) and human SH-SY5Y neuroblastoma cells at increasing concentrations (up to 3.0 μM) of squalamine, using confocal microscopy and anti–α-synuclein antibodies. The images were scanned at apical planes to detect oligomers (green channel) interacting with the cellular surface (red channel) (Fig. 3*C*). Large numbers of α-synuclein oligomers bound to the plasma membrane were observed in cells exposed to oligomers, but their number was markedly decreased as the squalamine concentration was increased (Fig. 3*C*). As we have shown previously, the toxicity caused by protein oligomers can be correlated with membrane binding (34) and this finding provides an explanation for the inhibition of the cellular damage induced by α-synuclein oligomers by squalamine and is consistent with a competitive binding model.

Squalamine Reduces α-Synuclein Aggregation and Related Paralysis in a Worm Model of PD. We extended our in vitro observations that squalamine can suppress the aggregation and toxicity of α-synuclein to a living system. We used a well-studied model of PD in the nematode worm *C. elegans*, which is based on the overexpression of α-synuclein tagged with yellow fluorescent protein (YFP) in the muscle cells of the nematode worms (25). This model organism, in which the presence of α-synuclein causes characteristic phenotypic changes (25), has been successfully used to probe the nature of a range of neurodegenerative conditions and has been used in high-throughput screens to identify novel genes that modify the course of disease (35, 36).

Motility in *C. elegans* declines during aging and it can be measured in liquid media by counting the number of body bends per unit of time (37). This phenotypic readout has been used extensively for identification of genes and pathways connected to age-related protein homeostasis, as well as for the definition of modifiers of protein aggregation (25, 35, 36); both of these processes are closely associated with the onset and development of neurodegenerative diseases (5, 7, 38). We first tested different approaches to optimize the effects of squalamine in vivo and found that the best treatment regime was to administer the compound at the larval stage L4, when the worms were fully developed, and to maintain the worms on plates seeded with squalamine for their whole lifespan. By carrying out standard

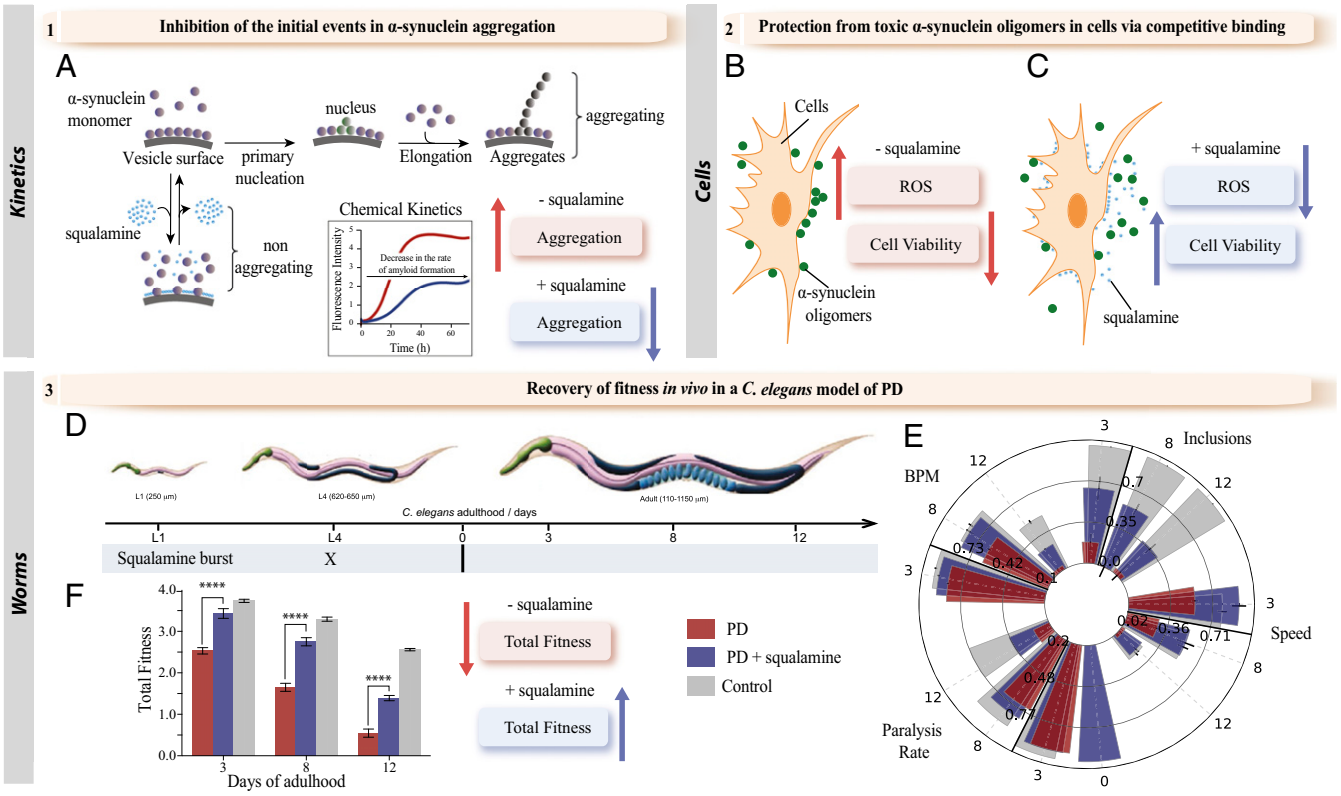

Fig. 6. Schematic illustration of the drug discovery strategy used in this work. (*A*) We used a wide range of biophysical techniques, including chemical kinetics, to study quantitatively the effects of squalamine on α-synuclein aggregation in vitro and we observed that squalamine affects the binding of α-synuclein to lipid membranes and inhibits the initial events in its aggregation. (*B* and *C*) By using the protocols that we recently developed to isolate oligomers of α-synuclein toxic to human cells (23, 24), we have shown that squalamine inhibits dramatically the mitochondrial dysfunction and cellular ROS production induced by the oligomers of α-synuclein (23, 24). (*D–F*) We further validated our results in vivo by using a well-established *C. elegans* model of PD (25), and we found that administration of a single dose of squalamine at the larval stage L4 (*D*) abolishes α-synuclein aggregation and its associated toxicity in vivo over several days (*E*) and increases the total fitness of the PD worms (*F*).

body bend assays (37), we observed a very significantly improved motility of the PD worms treated with squalamine (Fig. S4). By contrast, the motility of a *C. elegans* strain expressing only YFP, used here as a control, was not detectably affected by squalamine (Fig. S4).

As standard body bend assays monitored by manual means can be prone to errors and are not always reproducible, many digital tracking platforms have recently been proposed to characterize worm behavior in a more quantitative and rigorous way (39). To improve the reproducibility of the results, we have developed a high-throughput microscopic screening procedure that allows robust *C. elegans* phenotypic screening with improved statistics, coupled with automated analysis of the motility of the animals (see *SI Materials and Methods* for details).

Movies of swimming worms were recorded using a high-performance imaging lens and a machine vision camera at a high number of frames per second (fps) for 30 s or 1 min, and the platform enabled us to image simultaneously up to 200 swimming animals over the whole surface of a 6-cm agar plate (see *SI Materials and Methods* for details). Using this method, we confirmed with statistical confidence the observed improved motility (Fig. S5) of the PD worms upon squalamine administration (Figs. 4*A*, 5, and 6 and Movies S1–S4). Automated analysis of the velocities of the movements of the worms further confirmed a significant difference between treated and untreated PD worms, and indeed those animals exposed to 50 μM squalamine showed motility levels that were essentially the same as those of the control worms (Fig. 4*B*).

We then explored the effects of squalamine on the aggregation of α-synuclein in PD worms by fluorescence microscopy. Following the addition of squalamine to the medium in which the animals were maintained, we observed a substantial decrease in α-synuclein inclusion formation in aged PD worms (day 12 of adulthood) (Fig. 4 *C* and *D*), despite the fact that the levels of α-synuclein expression in the PD worms in the absence and in the presence of squalamine were found to be closely similar (Fig. 4*E*). We also demonstrated that no effects could be detected on the intensity or the distribution pattern of YFP expressed within the body-wall muscle of the control worms (Fig. 4*C*).

Furthermore the protective effect of squalamine was apparent throughout the study, as shown by recovery of motility (thrashing and speed), decrease in paralysis rate, and the decrease in the number of inclusions (Fig. 5). Finally, to assess whether or not the observed effects of squalamine in suppressing inclusion formation and toxicity were specific to the α-synuclein worms, we tested squalamine in a worm model of $A\beta_{42}$-mediated dysfunction (40). In this system, where the presence of lipids is not required for the initiation of $A\beta_{42}$ aggregation (41, 42), we observed that squalamine, at concentrations that completely restored the pathological phenotype in the $Abeta^{42}$ worms, showed no significant protective effects (Fig. S5), thereby indicating the specificity of squalamine against α-synuclein aggregation.

Discussion

We have shown by using a variety of biophysical techniques that squalamine can inhibit in vitro the aggregation of α-synuclein induced by lipid membranes. Furthermore we have shown by using a cellular model and an animal model of PD that squalamine dramatically reduces in vivo the toxicity associated with α-synuclein aggregation (Fig. 6).

To study the binding of α-synuclein to lipids, we first used SUVs composed of DOPS, DOPE, and DOPC, which are the most abundant lipids found in the membranes of synaptic vesicles (26). Titrating squalamine into a solution of α-synuclein bound to SUVs caused the α-helical content of α-synuclein to decrease in an approximately linear manner with squalamine concentration, as measured by CD and NMR, thus suggesting that squalamine displaces α-synuclein from lipid membranes, as observed for a range of other protein/lipid systems (17). We further explored the effects of squalamine on the binding and aggregation of α-synuclein in the presence of DMPS-containing vesicles, which have been shown to be particularly effective in enhancing the rate of aggregation and amyloid formation of α-synuclein (12). The presence of squalamine progressively decreased the α-helical content of α-synuclein, again indicating that this compound displaces the protein from the vesicles, as recently observed for β-synuclein (22). To analyze these data, we thus used the same competitive binding model as the one describing the inhibitory effect of β-synculein on α-synuclein lipid-induced aggregation (22), where both α-synuclein and squalamine compete for binding sites at the surface of the DMPS vesicles, which validated the model in a quantitative manner.

In addition, we have shown that squalamine does not interact directly with monomeric α-synuclein in free solution, except at very high concentrations and in the absence of lipids, and that it affects the size and the thermotropic properties of lipid vesicles only at high squalamine:DMPS ratios (>0.1). Moreover, we have observed that the overall rate of lipid-induced α-synuclein aggregation in vitro decreases dramatically and in a dose-dependent manner upon incubation with squalamine.

We then extended this study by using SH-SY5Y cells treated with oligomers of α-synuclein previously shown to be toxic to cells in culture (23, 24) and found that squalamine inhibits completely the mitochondrial dysfunction and the cellular ROS production induced by the oligomers. The degree of binding of toxic α-synuclein oligomers to neuronal cells also decreased with increasing squalamine concentration, and based on our results, we proposed a competitive binding model, where toxic oligomers of α-synuclein and squalamine compete for binding sites at the surface of neuronal cells. These results suggest that squalamine drastically decreases not only the neurotoxicity caused by the intracellular accumulation of α-synuclein aggregates but also the cellular damage induced by aggregates interacting with the membrane of neuronal cells. We then provided further evidence for a protective effect of squalamine observed in vitro and in cells by using a well-studied *C. elegans* model of PD (25). When worms were exposed to squalamine from an early stage in their development, we observed an almost complete recovery of the motility dysfunction induced by α-synuclein together with a substantial decrease in inclusion formation in treated PD worms.

Taken together, these results suggest that squalamine inhibits the initial step in the lipid-induced aggregation of α-synuclein through competitive binding at the surface of the lipid vesicles and also drastically reduces the toxicity of oligomeric forms of α-synuclein in vivo. We note that it is also possible that other secondary mechanisms of action, such as direct interactions with fibrils, may be present and could work in synergy with the principal mechanism of action of squalamine that we have described.

Conclusions

We have shown that in vitro and in cell cultures squalamine suppresses the initial events in the aggregation of α-synuclein by displacing the protein from lipid membranes, where such events preferentially take place, and also acts to reduce the interactions of oligomeric aggregates with the membrane surfaces (Fig. 6). These results indicate the mechanisms by which squalamine significantly inhibits the aggregation of α-synuclein in vivo and also reduces dramatically its associated toxicity. We suggest, therefore, that squalamine, and by extension other molecules that can compete effectively with α-synuclein for lipid membrane binding, could have the potential to act as therapeutic agents for PD and other conditions associated with the pathogenic aggregation of α-synuclein.

Materials and Methods

Extended experimental procedures are described in *SI Materials and Methods*. Wild-type α-synuclein was expressed in *Escherichia coli* and purified as previously described (10). DOPE/DOPS/DOPC vesicles were prepared as previously described (27). DMPS vesicles were prepared as previously reported (12) and

aggregation kinetics and related data analysis were carried out as previously described (12). α-Synuclein oligomers were also prepared as described previously (23, 24) and cell cytotoxicity assays were carried out as indicated (43). In vivo experiments were carried out by using a well-studied *C. elegans* model of PD (25).

ACKNOWLEDGMENTS. The authors thank Alfonso de Simone, Sam Casford, Mandy Koopman, and Maarten C. Hardenberg for valuable advice and discussions. This work was supported by the Intramural Research Program of the National Institute of Diabetes and Digestive and Kidney Diseases (NIDDK), US National Institutes of Health (A.M. and A.B.); by the Boehringer Ingelheim Fonds (P.F.); by a European Research Council starting grant (to M.B.D.M. and E.A.A.N.); and by The Cambridge Centre for Misfolding Diseases. N.C. thanks the Spanish Ministry of Economy and Competitiveness (RYC-2012-12068). S.W.C. thanks the Agency for Science, Technology, and Research, Singapore for support.

1. Breydo L, Wu JW, Uversky VN (2012) A-synuclein misfolding and Parkinson's disease. *Biochim Biophys Acta* 1822(2):261–285.
2. Dettmer U, Selkoe D, Bartels T (2016) New insights into cellular α-synuclein homeostasis in health and disease. *Curr Opin Neurobiol* 36:15–22.
3. Spillantini MG, Crowther RA, Jakes R, Hasegawa M, Goedert M (1998) alpha-Synuclein in filamentous inclusions of Lewy bodies from Parkinson's disease and dementia with lewy bodies. *Proc Natl Acad Sci USA* 95(11):6469–6473.
4. Dawson TM, Dawson VL (2003) Molecular pathways of neurodegeneration in Parkinson's disease. *Science* 302(5646):819–822.
5. Knowles TPJ, Vendruscolo M, Dobson CM (2014) The amyloid state and its association with protein misfolding diseases. *Nat Rev Mol Cell Biol* 15(6):384–396.
6. Gómez-Tortosa E, Ingraham AO, Irizarry MC, Hyman BT (1998) Dementia with Lewy bodies. *J Am Geriatr Soc* 46(11):1449–1458.
7. Chiti F, Dobson CM (2006) Protein misfolding, functional amyloid, and human disease. *Annu Rev Biochem* 75(1):333–366.
8. Tóth G, et al. (2014) Targeting the intrinsically disordered structural ensemble of α-synuclein by small molecules as a potential therapeutic strategy for Parkinson's disease. *PLoS One* 9(2):e87133.
9. Lee VMY, Trojanowski JQ (2006) Mechanisms of Parkinson's disease linked to pathological alpha-synuclein: New targets for drug discovery. *Neuron* 52(1):33–38.
10. Buell AK, et al. (2014) Solution conditions determine the relative importance of nucleation and growth processes in α-synuclein aggregation. *Proc Natl Acad Sci USA* 111(21):7671–7676.
11. Fink AL (2006) The aggregation and fibrillation of alpha-synuclein. *Acc Chem Res* 39(9):628–634.
12. Galvagnion C, et al. (2015) Lipid vesicles trigger α-synuclein aggregation by stimulating primary nucleation. *Nat Chem Biol* 11(3):229–234.
13. Habchi J, et al. (2016) An anticancer drug suppresses the primary nucleation reaction that initiates the production of the toxic Aβ42 aggregates linked with Alzheimer's disease. *Sci Adv* 2(2):e1501244.
14. Moore KS, et al. (1993) Squalamine: An aminosterol antibiotic from the shark. *Proc Natl Acad Sci USA* 90(4):1354–1358.
15. Li D, Williams JI, Pietras RJ (2002) Squalamine and cisplatin block angiogenesis and growth of human ovarian cancer cells with or without HER-2 gene overexpression. *Oncogene* 21(18):2805–2814.
16. Genaidy M, et al. (2002) Effect of squalamine on iris neovascularization in monkeys. *Retina* 22(6):772–778.
17. Yeung T, et al. (2008) Membrane phosphatidylserine regulates surface charge and protein localization. *Science* 319(5860):210–213.
18. Sumioka A, Yan D, Tomita S (2010) TARP phosphorylation regulates synaptic AMPA receptors through lipid bilayers. *Neuron* 66(5):755–767.
19. Alexander RT, et al. (2011) Membrane surface charge dictates the structure and function of the epithelial Na+/H+ exchanger. *EMBO J* 30(4):679–691.
20. Selinsky BS, Smith R, Frangiosi A, Vonbaur B, Pedersen L (2000) Squalamine is not a proton ionophore. *Biochim Biophys Acta* 1464(1):135–141.
21. Zasloff M, et al. (2011) Squalamine as a broad-spectrum systemic antiviral agent with therapeutic potential. *Proc Natl Acad Sci USA* 108(38):15978–15983.
22. Brown JWP, et al. (2016) β-Synuclein suppresses both the initiation and amplification steps of α-synuclein aggregation via competitive binding to surfaces. *Sci Rep* 6:36010.
23. Cremades N, et al. (2012) Direct observation of the interconversion of normal and toxic forms of α-synuclein. *Cell* 149(5):1048–1059.
24. Chen SW, et al. (2015) Structural characterization of toxic oligomers that are kinetically trapped during α-synuclein fibril formation. *Proc Natl Acad Sci USA* 112(16):E1994–E2003.
25. van Ham TJ, et al. (2008) C. elegans model identifies genetic modifiers of α-synuclein inclusion formation during aging. *PLoS Genet* 4(3):e1000027.
26. Takamori S, et al. (2006) Molecular anatomy of a trafficking organelle. *Cell* 127(4):831–846.
27. Bodner CR, Dobson CM, Bax A (2009) Multiple tight phospholipid-binding modes of alpha-synuclein revealed by solution NMR spectroscopy. *J Mol Biol* 390(4):775–790.
28. Wilhelm BG, et al. (2014) Composition of isolated synaptic boutons reveals the amounts of vesicle trafficking proteins. *Science* 344(6187):1023–1028.
29. Bussell R, Jr, Eliezer D (2004) Effects of Parkinson's disease-linked mutations on the structure of lipid-associated alpha-synuclein. *Biochemistry* 43(16):4810–4818.
30. Eliezer D, Kutluay E, Bussell R, Jr, Browne G (2001) Conformational properties of α-synuclein in its free and lipid-associated states. *J Mol Biol* 307(4):1061–1073.
31. Kosten J, et al. (2014) Efficient modification of alpha-synuclein serine 129 by protein kinase CK1 requires phosphorylation of tyrosine 125 as a priming event. *ACS Chem Neurosci* 5(12):1203–1208.
32. Serber Z, et al. (2006) Investigating macromolecules inside cultured and injected cells by in-cell NMR spectroscopy. *Nat Protoc* 1(6):2701–2709.
33. Fernández CO, et al. (2004) NMR of alpha-synuclein-polyamine complexes elucidates the mechanism and kinetics of induced aggregation. *EMBO J* 23(10):2039–2046.
34. Evangelisti E, et al. (2016) Binding affinity of amyloid oligomers to cellular membranes is a generic indicator of cellular dysfunction in protein misfolding diseases. *Sci Rep* 6:32721.
35. van Ham TJ, et al. (2010) Identification of MOAG-4/SERF as a regulator of age-related proteotoxicity. *Cell* 142(4):601–612.
36. van der Goot AT, et al. (2012) Delaying aging and the aging-associated decline in protein homeostasis by inhibition of tryptophan degradation. *Proc Natl Acad Sci USA* 109(37):14912–14917.
37. Gidalevitz T, Krupinski T, Garcia S, Morimoto RI (2009) Destabilizing protein polymorphisms in the genetic background direct phenotypic expression of mutant SOD1 toxicity. *PLoS Genet* 5(3):e1000399.
38. Soto C (2003) Unfolding the role of protein misfolding in neurodegenerative diseases. *Nat Rev Neurosci* 4(1):49–60.
39. Husson SJ, Costa WS, Schmitt C, Gottschalk A (2013) Keeping track of worm trackers. *WormBook* 1–17.
40. Link CD (1995) Expression of human beta-amyloid peptide in transgenic Caenorhabditis elegans. *Proc Natl Acad Sci USA* 92(20):9368–9372.
41. Cohen SIA, et al. (2013) Proliferation of amyloid-β42 aggregates occurs through a secondary nucleation mechanism. *Proc Natl Acad Sci USA* 110(24):9758–9763.
42. Scherzinger E, et al. (1999) Self-assembly of polyglutamine-containing huntingtin fragments into amyloid-like fibrils: Implications for Huntington's disease pathology. *Proc Natl Acad Sci USA* 96(8):4604–4609.
43. Cascella R, et al. (2013) Extracellular chaperones prevent Aβ42-induced toxicity in rat brains. *Biochim Biophys Acta* 1832(8):1217–1226.
44. Fusco G, et al. (2014) Direct observation of the three regions in α-synuclein that determine its membrane-bound behaviour. *Nat Commun* 5:3827.
45. Maltsev AS, Ying J, Bax A (2012) Impact of N-terminal acetylation of α-synuclein on its random coil and lipid binding properties. *Biochemistry* 51(25):5004–5013.
46. Bartels T, Kim NC, Luth ES, Selkoe DJ (2014) N-alpha-acetylation of α-synuclein increases its helical folding propensity, GM1 binding specificity and resistance to aggregation. *PLoS One* 9(7):e103727.
47. Anderson JP, et al. (2006) Phosphorylation of Ser-129 is the dominant pathological modification of α-synuclein in familial and sporadic Lewy body disease. *J Biol Chem* 281(40):29739–29752.
48. Johnson M, Coulton AT, Geeves MA, Mulvihill DP (2010) Targeted amino-terminal acetylation of recombinant proteins in E. coli. *PLoS One* 5(12):e15801–e15805.
49. Zhang X, et al. (1998) Synthesis of squalamine utilizing a readily accessible spermidine equivalent. *J Org Chem* 63(23):8599–8603.
50. Hoyer W, et al. (2002) Dependence of α-synuclein aggregate morphology on solution conditions. *J Mol Biol* 322(2):383–393.
51. Flagmeier P, et al. (2016) Mutations associated with familial Parkinson's disease alter the initiation and amplification steps of α-synuclein aggregation. *Proc Natl Acad Sci USA* 113(37):10328–10333.
52. Brenner S (1974) The genetics of Caenorhabditis elegans. *Genetics* 77(1):71–94.
53. Cohen E, Bieschke J, Perciavalle RM, Kelly JW, Dillin A (2006) Opposing activities protect against age-onset proteotoxicity. *Science* 313(5793):1604–1610.
54. Viswanathan M, Kim SK, Berdichevsky A, Guarente L (2005) A role for SIR-2.1 regulation of ER stress response genes in determining C. elegans life span. *Dev Cell* 9(5):605–615.
55. Lendel C, Bolognesi B, Wahlström A, Dobson CM, Gräslund A (2010) Detergent-like interaction of Congo red with the amyloid β peptide. *Biochemistry* 49(7):1358–1360.